Fermi surface contours obtained from scanning tunneling microscope images around surface

point defects

Fermi surface contours obtained from scanning tunneling microscope images around surface point defects

N V Khotkevych-Sanina[1]**, Yu A Kolesnichenko**[1,3]
and J M van Ruitenbeek[2]

[1] B I Verkin Institute for Low Temperature Physics and Engineering, National Academy of Sciences of Ukraine, 47, Lenin Avenue, 61103 Kharkov, Ukraine
[2] Kamerlingh Onnes Laboratorium, Universiteit Leiden, Postbus 9504, 2300 Leiden, The Netherlands
E-mail: kolesnichenko@ilt.kharkov.ua

Abstract. We present a theoretical analysis of the standing wave patterns in scanning tunneling microscope (STM) images, which occur around surface point defects. We consider arbitrary dispersion relations for the surface states and calculate the conductance for a system containing a small-size tunnel contact and a surface impurity. We find rigorous theoretical relations between the interference patterns in the real-space STM images, their Fourier transforms and the Fermi contours of two-dimensional electrons. We propose a new method for reconstructing Fermi contours of surface electron states, directly from the real-space STM images around isolated surface defects.

---

[3] Author to whom any correspondence should be addressed.

Contents

1. Introduction

Images obtained by scanning tunneling microscope (STM) on flat metal surfaces commonly display standing waves related to electron scattering by surface steps and single defects [1] (for a review see [2, 3]). The physical origin of the interference patterns in the constant-current STM images is the same as that of Friedel oscillations in the electron local density of states (LDOS) in the vicinity of a scatterer [4]. It is due to quantum interference between incident electron waves and waves scattered by the defects. Study of the standing wave pattern provides information on the defect itself and on the host metal. From the images the Fermi surface contours (FC) for two-dimensional (2D) surface states [2, 3, 5–12] and bulk Fermi surfaces can be studied [13–17].

Let us consider the question of the nature of the contour that we see in a real-space STM image. Can it be interpreted directly as the FC or some contour related to it? For isotropic (circular) FC the answer is obvious—the period of the conductance oscillations $\Delta r = 2\pi/2\kappa_F = \text{const}$ is set by twice the 2D Fermi wave vector, $2\kappa_F$. In the case of an anisotropic dispersion relation in real space the electrons move in the direction given by their velocity $\mathbf{v}_\kappa$, which need not be parallel to the wave vector κ. We expect that, similar to the problem of subsurface defects in the bulk [13, 14], the period of the real-space oscillatory pattern is $\Delta r = 2\pi/2\kappa_F \mathbf{n}_0$, where $\mathbf{n}_0$ is the 2D unit vector pointing from the defect to the position of the tip apex and κ_F is the Fermi wave vector, the magnitude of which depends on its direction. Thus, in the STM image we observe a curve shaped by the projection of the wave vector κ_F on the normal to the FC. In the case of large anisotropy this contour may be very different from the FC itself. In [2, 3, 5–12] Fourier transforms (FT) of STM images of wave patterns around surface point defects were interpreted as FC. We are not aware of any rigorous mathematical justification of this procedure. Is there another way of reconstructing the true FC from real-space STM images? The answer to this question is the main aim of this paper.

The STM theory used most frequently by experimentalists is the approach of Tersoff and Hamann [18]. Their theoretical analysis of the tunnel current is based on Bardeen's approximation [19], in which a tunneling matrix element is calculated using the decay of the wave functions of the two individual (isolated) electrodes inside the barrier. For the STM tip they adopt a model of angle-independent wave functions and the surface states are described

by Bloch wave functions, which decay exponentially inside the tunnel barrier. Tersoff and Hamann [18] found that the STM conductance is directly proportional to the electron LDOS $\rho(\mathbf{r})$ at a point $\mathbf{r} = \mathbf{r}_0$, at the position of the contact. In the same spirit, the influence on the STM conductance of adatoms or defects embedded into the sample surface is usually described by their influence on the 2D LDOS. This was used, for example, to explain the observation of a 'quantum mirage' in 'quantum corrals' [20] in terms of a free-electron approximation, and for the interpretation of the anisotropic standing Bloch waves observed on Be surfaces [3, 10]. In spite of the large number of theoretical works dealing with STM theory (for a review see [21, 22]), a number of questions about the theoretical description of anisotropic standing wave patterns in STM images remain poorly described.

The main new points of present paper are: (i) in an approximation of free electrons with an arbitrary anisotropic dispersion law the quantum electron tunneling through a small contact into Shockley-like 2D surface states is considered theoretically. In the framework of a model of an inhomogeneous δ-like tunnel barrier, [23, 24], we obtain analytical formulas for the conductance G of the contact in the presence of a single defect incorporated in the sample surface. (ii) We formulate a rigorous mathematical procedure for the FC reconstruction from real-space images of conductance oscillations around surface point-like defects in terms of a support function of a plane curve (see e.g. [27]).

The organization of this paper is as follows. The model that we use to describe the contact and the basic equations are presented in section 2. In section 3 the differential conductance is found on the basis of a calculation of the probability current density through the contact. Section 4 presents the mathematical procedure of reconstruction of FC in the momentum space from the real-space image. In section 5 we conclude by discussing the possibilities for exploiting these theoretical results for interpretation of STM experiments. In appendix A the method for obtaining a solution of the Schrödinger equation is described, and in appendix B we find the asymptote of the 2D electron Green's function for large values of the coordinates, which is necessary to describe the conductance oscillations at large distances between the tip and the defect.

2. Model of the system and basic equations

The STM tip and a conducting surface form an atomic size tunnel contact. The STM image is obtained from the height profile while maintaining the tunnel current I constant, or from the differential conductance $G = \mathrm{d}I/\mathrm{d}V$) measured as a function of the lateral coordinates. Such dependences are a kind of electronic 'map' of the surface, thereby they show a variety of defects situated on the metal's surface (adsorbed and embedded impurities, steps, etc) We focus our attention on studying the shape of contours of oscillatory patterns around a single point defect. These concentric contours centered on the defect (see figure 1) are minima and maxima of the oscillatory dependence of the conductance on the lateral coordinates.

In [24] it was proposed to model the STM experiments by an inhomogeneous infinitely thin tunnel barrier. The important simplification offered by this model is the replacement of the three-dimensional inhomogeneous tunnel barrier in a real experimental configuration by a 2D one. In the present paper we use this model to describe the interference pattern around a point defect resulting from electron surface states having an anisotropic FC. Instead of a description by
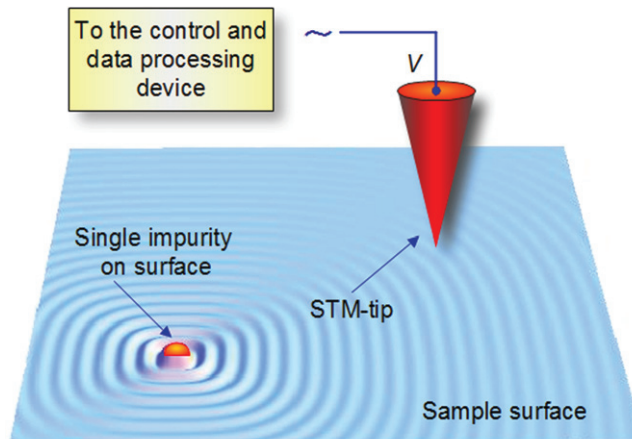
Figure 1. Schematic setup for measurements with a STM. A standing wave pattern arising around a single impurity on the surface is shown.
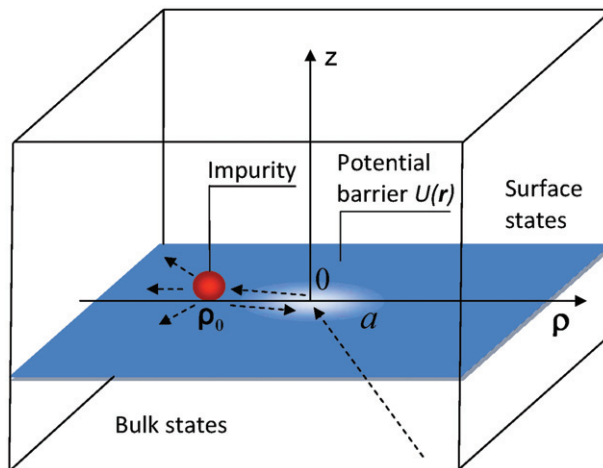

Figure 2. Illustration of the model used for the description of STM tunneling into the surface states. The blue colored region of the interface at $z = 0$ separates the tip (lower half) from the sample (upper half). In the center of the interface at the point $\mathbf{r} = 0$ a region is shown having maximal probability of electron tunneling, which models a contact of characteristic radius a. At the point $\mathbf{r} = (\boldsymbol{\rho}_0, z_0)$ a point-like defect is situated. Arrows schematically show semiclassical trajectories of electrons, for the bulk states in the half-space $z < 0$, and for the surface electrons at $z > 0$.

means of simple Bloch waves we consider quasiparticles [25] for conduction electrons having arbitrary dispersion relations.

The model that we consider is presented in figure 2. Two conducting half-spaces are separated by an infinitely thin insulating interface at $z = 0$, the potential barrier $U(\mathbf{r})$ in the plane of which we describe by Dirac delta function $U(\mathbf{r}) = U_0 f(\boldsymbol{\rho}) \delta(z)$. A dimensionless function $f(\boldsymbol{\rho})$ describes a barrier inhomogeneity in the plane $\boldsymbol{\rho} = (x, y)$. This inhomogeneity simulates the STM tip and provides the path for electron tunneling through a bounded region of scale

$a \lesssim \lambda_F$ (a is the characteristic radius of the contact, λ_F is the electron Fermi wavelength), i.e. the function $f(\boldsymbol{\rho})$ must have the property

$$f(\boldsymbol{\rho}) = \begin{cases} \sim 1, & \rho \lesssim a, \\ \to \infty, & \rho \gg a. \end{cases} \tag{1}$$

Simple examples of such a function are $f(\boldsymbol{\rho}) = \exp(\rho^2/a^2)$ and $1/f(\boldsymbol{\rho}) = \Theta(a - \rho)$, where $\Theta(x)$ is the Heaviside step function. The latter function corresponds to a model with a circular orifice of radius a in an otherwise impenetrable interface.

Shockley-like surface states are included in the model by means of a surface potential $V_{sur}(z)$ in the half-space $z > 0$. The potential $V_{sur}(z)$ and the barrier at $z = 0$ form a quantum well which localizes electrons near the surface. A specific form of the function $V_{sur}(z)$ is not important for us. It is enough to assume that $V_{sur}(z)$ is an analytic monotonic function such that it permits the existence of one and only one surface state in the region $z > 0$ below the Fermi energy ε_F. The surface state localization length l is assumed to be much larger than the characteristic contact diameter, $a \ll l$.

A single point-like defect is placed at a point $\mathbf{r}_0 = (\boldsymbol{\rho}_0, z_0 > 0)$ in the vicinity of the interface at $z = 0$. The electron scattering by the defect we describe by a short-range potential $D(\mathbf{r}) = g D_0(\mathbf{r} - \mathbf{r}_0)$ localized within a region of characteristic radius r_D, and in the half-space $z > 0$, around the point $\mathbf{r}_0 = (\boldsymbol{\rho}_0, z_0)$, where g is the constant measuring the strength of the electron interaction with the defect. It satisfies the normalization condition

$$\int_{-\infty}^{\infty} d\mathbf{r} D_0(\mathbf{r} - \mathbf{r}_0) = 1. \tag{2}$$

We do not specify the concrete form of the potential $D(\mathbf{r})$. The specific form affects the amplitude and phase of the conductance oscillations but it does not change their period, which is the main subject of interest for us. We assume the following general properties for this function: (i) the potential is repulsive and electron bound states near the defect are absent; (ii) the constant of interaction g in the potential $D(\mathbf{r})$ is small such that Born's approximation for waves scattered by the defect is applicable; (iii) the effective radius r_D of the potential $D(\mathbf{r})$ is small enough $\kappa_F r_D \ll 1$ for the scattering to be described in the s-wave approximation. All of the listed conditions can be easily satisfied in experiments.

In order to obtain an analytical solution of the Schrödinger equation and calculate the electric current in what follows we use a simplified model for the anisotropic dispersion law $\varepsilon(\mathbf{k})$ for the charge carriers

$$\varepsilon(\mathbf{k}) = \varepsilon_{2D}(\boldsymbol{\kappa}) + \frac{\hbar^2 k_z^2}{2m_z}, \tag{3}$$

where $\boldsymbol{\kappa}$ is the 2D electron wave vector in the plane of interface, $\varepsilon_{2D}(\boldsymbol{\kappa})$ is an arbitrary function describing the energy spectrum of the surface states and m_z is the effective mass characterizing the electron motion along the normal to the interface.

The wave function ψ satisfies the Schrödinger equation

$$\left(\varepsilon_{2D}\left(\frac{\hbar \partial}{i \partial \boldsymbol{\rho}} \right) + \frac{\hbar^2 \partial^2}{2m_z \partial z^2} \right) \psi(\mathbf{r}) + [\varepsilon - U(\mathbf{r}) - D(\mathbf{r}) - V_{sur}(z)\Theta(z)] \psi(\mathbf{r}) = 0 \tag{4}$$

with ε the electron energy. At the interface $z = 0$ the function $\psi(\mathbf{r})$ satisfies the boundary conditions for continuity of the wave function

$$\psi(\boldsymbol{\rho}, +0) = \psi(\boldsymbol{\rho}, -0) \tag{5}$$

and jump of its derivative

$$\psi'_z(\boldsymbol{\rho}, +0) - \psi'_z(\boldsymbol{\rho}, -0) = \frac{2m_z U_0}{\hbar^2} f(\boldsymbol{\rho}) \psi(\boldsymbol{\rho}, 0) \tag{6}$$

and the condition for the decay of the surface state wave function in the classically forbidden region

$$\psi(\boldsymbol{\rho}, z \to \infty) \to 0. \tag{7}$$

For $z \to -\infty$ the solution $\psi(\mathbf{r})$ of equation (4) must describe waves emanating from the contact [13]

$$\psi(|\mathbf{r}| \to \infty, z < 0) \sim \frac{\exp(\mathrm{i}k\mathbf{n}r)}{r}, \tag{8}$$

where $\mathbf{n}$ is a unit vector directed along the velocity vector $\mathbf{v_k} = \partial \varepsilon(\mathbf{k})/\partial \mathbf{k}$.

In order to calculate the tunnel current at small applied voltage V ($eV \ll \varepsilon_F$) we must find the wave function $\psi_{tr}(\boldsymbol{\rho}, z)$ for electrons transmitted through the tunnel barrier. By means of this function the density of current flow and the total current in the system can be calculated. At zero temperature it is enough to consider one direction of tunneling. For definiteness we select the sign of the voltage such that the tunneling occurs from the surface states at $z > 0$ into the bulk states at $z < 0$ (see figure 3). The total current I can be found by the integration over the wave vectors $\boldsymbol{\kappa}$ of the surface states and integration over coordinate $\boldsymbol{\rho}$ in the plane $z = \mathrm{const} \neq 0$ in the half-space $z < 0$

$$I = -\frac{e^2 \hbar L_x L_y V}{2\pi^2 m_z} \int_{-\infty}^{\infty} \mathrm{d}\kappa \int_{-\infty}^{\infty} \mathrm{d}\boldsymbol{\rho} \, \mathrm{Im} \left[\psi_{tr}^*(\boldsymbol{\rho}, z) \frac{\partial}{\partial z} \psi_{tr}(\boldsymbol{\rho}, z) \right] \frac{\partial f_F(\varepsilon)}{\partial \varepsilon}. \tag{9}$$

Here $L_{x,y}$ is the size of the sample in the corresponding direction.

The procedure for the solution of the Schrödinger equation (4) with boundary conditions (5)–(8) is presented in appendix A, where the wave function $\psi_{tr}(\boldsymbol{\rho}, z)$ (A.17) is found.

3. Standing wave pattern in the conductance of a small contact

Obviously, in the case of small applied bias which we consider in this work, $|eV| \ll \varepsilon_F$, with ε_F the Fermi energy, the conductance $G = I/V$ does not depend on the direction of the current. Substituting the wave function $\psi_{tr}(\boldsymbol{\rho}, z)$ (A.17) in equation (9) after some integrations we find

$$G = \frac{e^2 \hbar^5 \left| \chi'_{0z}(+0) \right|^2}{32\pi^4 m_z^3 U_0^2} \int_{-\infty}^{\infty} \int_{-\infty}^{\infty} \frac{\mathrm{d}\boldsymbol{\rho}'}{f(\boldsymbol{\rho}')} \frac{\mathrm{d}\boldsymbol{\rho}''}{f(\boldsymbol{\rho}'')} \int_0^{\infty} \mathrm{d}\kappa' k_z' \Theta \left(\varepsilon_F - \varepsilon_{2D} \left(\kappa' \right) \right) \cos \left[\kappa' \left(\boldsymbol{\rho}' - \boldsymbol{\rho}'' \right) \right]$$

$$\times \int_0^{\infty} \mathrm{d}\kappa \cdot \delta \left(\varepsilon_F - \varepsilon_{2D}(\kappa) - \varepsilon_0 \right) \left[\cos \left[\kappa \left(\boldsymbol{\rho}' - \boldsymbol{\rho}'' \right) \right] \right]$$
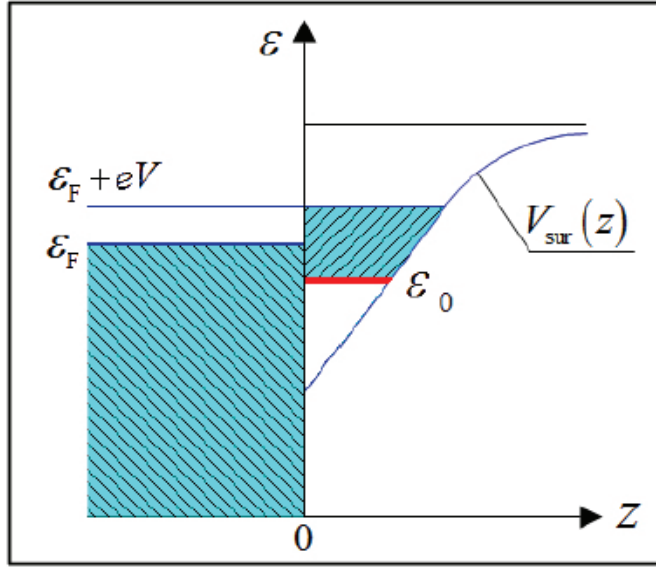
Figure 3. Illustration of the occupied energy bands near the interface. The applied bias eV makes it possible for the electrons to tunnel from surface states into bulk states of the STM tip.

$$+2g \int_{-\infty}^{\infty} d\boldsymbol{\rho}''' \int_{-\infty}^{\infty} dz''' D_0\big(\boldsymbol{\rho}''' - \boldsymbol{\rho}_0, z''' - z_0\big) \big|\chi_0\big(z'''\big)\big|^2$$

$$\times \cos\big[\kappa\big(\boldsymbol{\rho}' - \boldsymbol{\rho}'''\big)\big] \mathrm{Re} G_{2D}^+ \big(\boldsymbol{\rho}' - \boldsymbol{\rho}'''; \varepsilon_F - \varepsilon_0\big)\big]. \tag{10}$$

Further calculations require explicit expressions for the functions $f(\boldsymbol{\rho})$ and $D_0(\boldsymbol{\rho} - \boldsymbol{\rho}_0, z - z_0)$. The integral formula (10) can be simplified for contacts of small radius a and in the limit of a short range r_D of the scattering potential. If $\kappa_F a \ll 1$ and $\kappa_F r_D \ll 1$, where $\kappa_F = \frac{1}{\hbar}\sqrt{2m_z(\varepsilon_F - \varepsilon_0)}$, all functions in (10) under the integrals, except $f(\boldsymbol{\rho})$ and $D_0(\boldsymbol{\rho} - \boldsymbol{\rho}_0, z - z_0)$, can be taken at the points $\boldsymbol{\rho}' = \boldsymbol{\rho}'' = 0$, $\boldsymbol{\rho}''' = \boldsymbol{\rho}_0$, which simplifies (10) to

$$G = G_0\left[1 + \frac{2\tilde{g}}{(2\pi\hbar)^2\,\rho_{2D}(\varepsilon_F - \varepsilon_0)}\mathrm{Re} G_{2D}^+\big(\boldsymbol{\rho}_0; \varepsilon_F - \varepsilon_0\big)\oint_{\varepsilon_F - \varepsilon_0 = \varepsilon_{2D}(\kappa)}\frac{dl_\kappa}{v_\kappa}\cos\kappa\boldsymbol{\rho}_0\right]. \tag{11}$$

Here

$$G_0 = \frac{e^2\hbar^5\,\big|\chi'_{0z}(+0)\big|^2}{8m_z^3 U_0^2}S_{\mathrm{eff}}^2\rho_{2D}(\varepsilon_F - \varepsilon_0)\Omega(\varepsilon_F) \tag{12}$$

is the conductance of a tunnel point contact between the surface states, unperturbed by defects, and the bulk states of the tip. Further,

$$\rho_{2D}(\varepsilon) = \frac{2}{(2\pi\hbar)^2}\oint_{\varepsilon = \varepsilon_{2D}(\kappa)}\frac{dl_\kappa}{v_\kappa} \tag{13}$$

is the 2D density of states, where the integration is carried out over the arc length l_κ of the constant-energy contour, $v_\kappa = |\partial \varepsilon_{2D}(\boldsymbol{\kappa})/\hbar \partial \boldsymbol{\kappa}|$ is the absolute value of the 2D velocity vector

$$\Omega(\varepsilon) = \frac{\sqrt{2m_z}}{\hbar} \int_0^\varepsilon d\varepsilon' \sqrt{\varepsilon - \varepsilon'} \rho_{2D}(\varepsilon'), \tag{14}$$

$$S_{\text{eff}} = \int_{-\infty}^\infty \frac{d\boldsymbol{\rho}}{f(\boldsymbol{\rho})} \tag{15}$$

is the effective area of the contact, and

$$\widetilde{g} = g \int_{-\infty}^\infty d\boldsymbol{\rho} \int_0^\infty dz \, D_0(\boldsymbol{\rho}, z - z_0) |\chi_0(z)|^2 \tag{16}$$

is the effective constant of interaction with the defect for the electrons belonging to the surface states.

For large distances between the contact and the defect, $\kappa_F \rho_0 \gg 1$, equation (11) can be reduced by using an asymptotic expression for the Green function, see (B.15) in appendix B. The asymptotic form for $\kappa_F \rho_0 \gg 1$ of the integral over l_κ in equation (11) is the real part of equation (B.3). Under the assumptions listed above the formula for the oscillatory part of the conductance takes the form

$$\frac{G_{\text{osc}}(\boldsymbol{\rho}_0)}{G_0} = \widetilde{g} \left. \frac{\text{sgn} K(\boldsymbol{\kappa}) \cos(2\boldsymbol{\kappa} \boldsymbol{\rho}_0)}{2\rho_{2D}(\varepsilon)\hbar^2 v_\kappa^2 |K(\boldsymbol{\kappa})| \rho_0} \right|_{\boldsymbol{\kappa} = \boldsymbol{\kappa}(\varepsilon_F - \varepsilon_0, \phi_0)}, \tag{17}$$

where ϕ_0 satisfies the stationary phase condition (B.8) for $\rho = \rho_0$. We emphasize that the result (17) is valid if $\kappa_F a \ll 1 \ \kappa_F r_D \ll 1$ and $\kappa_F \rho_0 \gg 1$. For example, in actual STM experiments for surface states of Cu (111) [1] the Fermi wave vector is $\kappa_F \simeq 0.2 \, \text{Å}^{-1}$, while a and r_D are of atomic size $a \simeq r_D \simeq 1 \, \text{Å}$. The period of real-space conductance oscillations is $\Delta\rho_0 \simeq \pi/\kappa_F \simeq 15 \, \text{Å}$ and the distance over which these oscillations are observable reaches $\rho_0 \simeq 100 \, \text{Å}$. Note that the asymptotic form (17) can be used to describe experimental data with satisfactory accuracy, with the less strict requirements of a and r_D smaller than the Fermi wavelength $\lambda_F = 2\pi/\kappa_F$, and $\kappa_F \rho_0 > 1$.

In [26] the expression for the conductance (10) has been found for the special case of an elliptic Fermi surface for the surface charge carriers. Within that model the conductance oscillations G_{osc} can be evaluated correctly in a wider interval of values for $\kappa_F \rho_0$, including $\kappa_F \rho_0 \lesssim 1$ (but $\rho_0 \gg a, r_D$). A comparison of that result with the asymptotic formula (17) for an elliptic Fermi contour shows that the relative error in the period of oscillations $\Delta\rho_0$ determined, as an example, as the distance between the third and fourth maxima in the dependence $G_{\text{osc}}(\boldsymbol{\rho}_0)$ (17) is about a few per cent.

4. Reconstruction of the Fermi contour from real-space scanning tunneling microscope images

Above we have shown that for large distances between the contact and the defect the period of the oscillations in the conductance is defined by the function $\boldsymbol{\kappa}(\varepsilon_F, \phi_0)\boldsymbol{\rho}_0$. Taking into account that according to equation (B.8) in the stationary phase point $\boldsymbol{\kappa} = \boldsymbol{\kappa}(\varepsilon, \phi_0)$ the vector $\boldsymbol{\rho}_0$ is
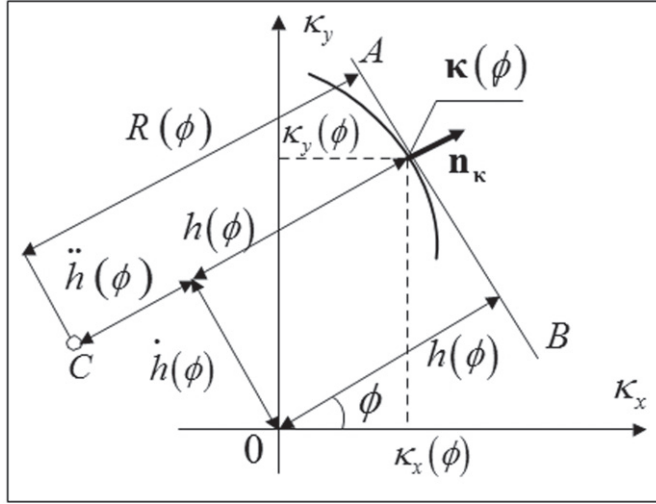
Figure 4. Geometric relations between the coordinates $\kappa_x(\phi)$ and $\kappa_y(\phi)$ of the parametrically defined convex curve and the support function $h(\phi)$ and its derivatives $\dot{h}(\phi)$, $\ddot{h}(\phi)$ with respect to the angle ϕ, the radius of curvature $R(\phi)$, and the normal vector $\mathbf{n}_\kappa$ at the point $\kappa(\phi)$. AB is the tangent to the curve in the point $\kappa(\phi)$.

parallel to the electron velocity, $\boldsymbol{\rho}_0 \parallel \mathbf{v}_\kappa(\varepsilon_F, \phi_0)$, i.e.

$$\boldsymbol{\kappa}(\varepsilon_F, \phi_0)\boldsymbol{\rho}_0 = \kappa\mathbf{n}_\kappa\rho_0 = h(\varepsilon_F, \phi_0)\rho_0, \tag{18}$$

where $\mathbf{v}_\kappa/v_\kappa = \mathbf{n}_\kappa$ is the unit vector normal to the contour of constant energy $\varepsilon_{2D}(\mathbf{q}) = \varepsilon_F - \varepsilon_0$ in the point defined by wave vector $\boldsymbol{\kappa}$.

By definition $h(\phi) = \boldsymbol{\kappa}\mathbf{n}_\kappa > 0$, the distance of the tangent from the origin, is the support function for a convex plane curve [27]. In figure 4 we illustrate the geometrical relation between the curve and its support function. For known $h(\phi)$ and its first and second derivatives, $\dot{h}(\phi)$ and $\ddot{h}(\phi)$, the convex plane curve is given by the parametric equations [27]

$$\kappa_x(\phi) = h(\phi)\cos\phi - \dot{h}(\phi)\sin\phi, \tag{19}$$

$$\kappa_y(\phi) = h(\phi)\sin\phi + \dot{h}(\phi)\cos\phi \tag{20}$$

and the radius of curvature $R(\phi)$ is

$$R(\phi) = h(\phi) + \ddot{h}(\phi). \tag{21}$$

The curvature is $K(\phi) = 1/R(\phi)$. Obviously, for a circle $|\boldsymbol{\kappa}|$ is constant and the support function coincides with the circle radius, $h = \kappa$.

Maxima and minima in the oscillatory dependence of the conductance are the curves of constant phase of the oscillatory functions in equation (17), $2h(\phi_0)\rho_0 = \text{const}$, and visible contours are defined by the function

$$\rho_0(\phi_0) = \frac{\text{const}}{2h(\phi_0)}. \tag{22}$$

Thus, equations (19), (20) and (22), in principle, offer the possibility of FC reconstruction from the real-space images. For a non-convex contour $\rho_0(\phi_0)$ (22) may be separated on parts having a constant sign of curvature and for each of them the above described procedure of reconstruction can be applied.

In order to answer the question what contour is obtained from the FT $F(\mathbf{q})$ of an STM image, we analyze equation (17). Although (17) is strictly valid only for $\kappa_F \rho_0 \gg 1$ in the region $\kappa_F \rho_0 > 1$ the difference of the true period $\Delta\rho_0$ of the oscillations from the value $\Delta\rho_0 = \pi/h(\phi_0)$ is small, as mentioned for an elliptic Fermi contour above. Performing the FT we find

$$(2\pi)^2 F(\mathbf{q}) = \int_0^\infty \mathrm{d}\rho\rho \int_0^{2\pi} \mathrm{d}\phi \frac{\cos(2h(\phi)\rho)}{\rho} \exp(\mathrm{i}Q(\phi)\rho) \qquad (23)$$

$$= \frac{\pi}{2}\left[\frac{1}{2\dot{h}(\phi_1) - \dot{Q}(\phi_1)} + \frac{1}{2\dot{h}(\phi_2) + \dot{Q}(\phi_2)}\right] - \mathrm{i}\int_0^{2\pi} \mathrm{d}\phi \frac{Q(\phi)}{Q^2(\phi) - 4h^2(\phi)},$$

where

$$Q(\phi) = (q_x \cos\phi + q_y \sin\phi) \qquad (24)$$

and $\phi_{1,2} = \phi_{1,2}(q_x, q_y)$ are the solutions of the equations

$$2h(\phi_{1,2}) = \pm Q(\phi_{1,2}). \qquad (25)$$

The function $F(\mathbf{q})$ (24) has a singularity when

$$2\dot{h}(\phi_{1,2}) = \pm\dot{Q}(\phi_{1,2}). \qquad (26)$$

From equations (19) and (20) it follows that for κ_x and κ_y belonging to a contour of constant energy

$$\kappa_x \cos\phi + \kappa_y \sin\phi = h(\phi) > 0, \qquad (27)$$

$$\kappa_x \sin\phi - \kappa_y \cos\phi = -\dot{h}(\phi). \qquad (28)$$

It is easy to see that simultaneous fulfillment of the conditions (25) and (26) at $\phi = \phi_1$ is equivalent to equations (27) and (28), which are the parametric equations of the constant energy contour, i.e. the FT gives the doubled FC of the surface state electrons. The solution $\phi = \phi_2$ of the second equation corresponds to the reflection symmetry point $-\mathbf{q} = (-q_x, -q_y)$ of the 2D Fermi surface.

Figure 4(a) illustrates the standing wave pattern in the conductance $G(\boldsymbol{\rho}_0)$ (17) around the defect for a model FC, which we take to be a convex curve described by the support function [29]

$$h(\phi) = k_0(\cos^2 2\phi + 8). \qquad (29)$$

In the absence of spin–orbit interaction the 2D Fermi surface has a center of symmetry $\varepsilon(\boldsymbol{\kappa}) = \varepsilon(-\boldsymbol{\kappa})$ and also the contour described by the support function $h(\phi)$ (29) acquires this property, $h(\phi) = h(\phi + \pi)$. The parametric equations of the curve in figure 4 can be easily found from equations (19) and (20). Figure 4(b) shows the difference between the true form of the curve and its support function.

The relation between contours of constant phase $\rho_0 = \mathrm{const}/2h(\phi)$ in the oscillatory pattern of the conductance (17) in figure 5(a) and the FC in figure 5(b), can be understood as follows [13]. For an anisotropic FC the surface electrons move along the direction of the
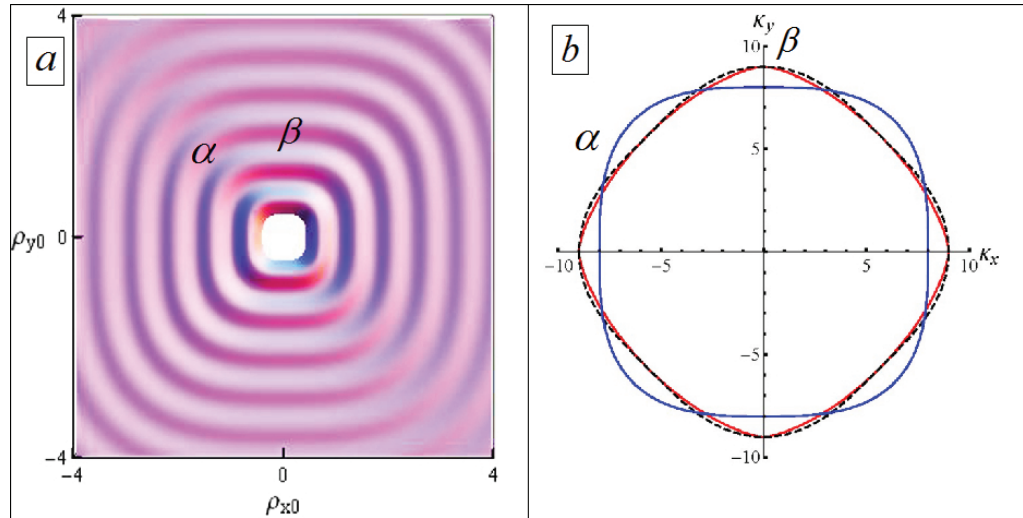
Figure 5. (a) Interference pattern in the conductance G as obtained from equation (17) resulting from scattering of the electrons by a surface defect. The coordinates ρ_{x0} and ρ_{y0} are given in units of $1/k_0$. The support function is given by equation (29). (b) Plots of the Fermi contour (solid), its support function h (short-dashed) and $1/h$ (long-dashed) with κ_x and κ_y in units of k_0.

velocity vector $\mathbf{v}_\kappa$, which need not generally be parallel to the wave vector κ. The standing wave at any point of the STM image is defined by the velocity directed from the contact to the defect. For parts of the FC having a small curvature (illustrated by the point α in figure 5(b)) all electrons for different κ in this region have similar velocities. In real space together they form a narrow electron beam and contribute to only a small sector of the STM image. Conversely, for electrons belonging to small parts of the FC having a large curvature (illustrated by the point β in figure 5), a small change of the angle ϕ (and consequently a small change of $\mathbf{k}(\phi)$) results in a large change in the direction of the velocity. Such small parts of the FC define large sectors in the interference pattern. We emphasize that, despite the resemblance, the contours of constant phase in $G(\boldsymbol{\rho}_0)$ are not just rotated Fermi contours.

5. Conclusion

In summary, we have investigated the conductance of a small-size tunnel contact for the case of electron tunneling from surface states into bulk states of the 'tip'. Electron scattering by a single surface defect is taken into account. For an arbitrary shape of the Fermi contour of the 2D surface states, an asymptotically exact formula for the STM conductance is obtained, in the limit of a high tunnel barrier and large distances between the contact and the defect. The relation between the standing wave pattern in the conductance and the geometry of 2D Fermi contour is analyzed. We show that the real-space STM image does not show the Fermi surface directly, but gives the contours of the inverse support function $1/h$ of the 2D Fermi contour. A rigorous mathematical procedure for the FC reconstruction from the real-space STM images is described.

Today STM imaging has become a new method of fermiology. By using FT scanning tunneling spectroscopy the FC may be found from the standing wave pattern of the electrons near the Fermi energy, caused by defects in the surface. To establish a correspondence between the observed contours and the actual FC, various theoretical approaches have been proposed (for a review of experimental and theoretical results on this subject see [3]). However, in some cases (see e.g. figure 2 in [7]) such a correspondence is not obvious. We propose another approach, which was very fruitful in bulk metal physics [25]—experimental results are compared with theoretical formulas obtained for arbitrary Fermi surfaces—i.e. the inverse problem of the Fermi surface reconstruction from the experimental data must be solved. The formulas obtained in this papers for oscillations of the conductance of the tunnel point contact around point-like surface defects and the procedure of the FC reconstruction directly from real-space STM image is a more rigorous alternative to the FT of STM images.

Appendix A. Solution of the Schrödinger equation

We search for the solution of equation (4) corresponding to electron tunneling from the surface states at $z > 0$ into the bulk states in the half-space $z < 0$. Hereinafter we follow the procedure for finding the wave function of transmitted electrons $\psi_{\text{tr}}(\boldsymbol{\rho}, z)$ in the limits $U_0 \to \infty$, $g \to 0$ that was proposed in [23, 24]. The wave function of surface states $\psi_{\text{sur}}(\boldsymbol{\rho}, z)$ at $z \geqslant 0$ we search as a sum

$$\psi_{\text{sur}}(\mathbf{r}) \simeq \varphi_{0\text{sur}}(\mathbf{r}) + \frac{1}{U_0}\varphi_{1\text{sur}}(\mathbf{r}), \tag{A.1}$$

where the second term is a small perturbation of surface state due to finite probability of tunneling through the contact. In approximation to zeroth order in $1/U_0$ the electrons cannot tunnel through the barrier and the function $\varphi_{0\text{sur}}(\mathbf{r})$ satisfies the zero boundary condition

$$\varphi_{0\text{sur}}(\boldsymbol{\rho}, z = 0) = 0. \tag{A.2}$$

The wave function of transmitted electrons $\psi_{\text{tr}}(\boldsymbol{\rho}, z)$ is not zero to first order in $1/U_0$

$$\psi_{\text{tr}}(\mathbf{r}) \simeq \frac{1}{U_0}\varphi_{1\text{tr}}(\mathbf{r}). \tag{A.3}$$

Substituting equations (A.1) and (A.3) in the boundary conditions (5), (6) and equating the terms of the same order in $1/U_0$ we obtain the boundary conditions

$$\varphi_{1\text{sur}}(\boldsymbol{\rho}, +0) = \varphi_{1\text{tr}}(\boldsymbol{\rho}, -0), \tag{A.4}$$

$$\left.\frac{\partial}{\partial z}\varphi_{0\text{sur}}(\boldsymbol{\rho}, z)\right|_{z=0} = \frac{2m_z}{\hbar^2}f(\boldsymbol{\rho})\varphi_{1\text{tr}}(\boldsymbol{\rho}, 0). \tag{A.5}$$

The function $\varphi_{0\text{sur}}(\boldsymbol{\rho}, z)$ will be found in linear approximation in the constant g. The unperturbed wave function (in the zeroth approximation in $1/U_0$ and g) $\varphi_{00\text{sur}}(\boldsymbol{\rho}, z)$ can be easily found

$$\varphi_{00\text{sur}}(\boldsymbol{\rho}, z) = \frac{1}{\sqrt{L_x L_y}}\,e^{i\boldsymbol{\kappa}\boldsymbol{\rho}}\chi_0(z). \tag{A.6}$$

In equation (A.6) $L_x \simeq L_y$ are the lateral sizes of the interface ($L_{x,y} \to \infty$), and $\chi_0(z)$ is the solution to the equation

$$\frac{\hbar^2}{2m_z} \frac{\partial^2 \chi_0(z)}{\partial z^2} + (\varepsilon_0 - V_{\text{sur}}(z)) \chi_0(z) = 0, \quad z \geqslant 0 \tag{A.7}$$

subject to the boundary conditions and normalization condition

$$\chi_0(0) = 0, \quad \chi_0(z \to \infty) \to 0, \tag{A.8}$$
$$\int_0^\infty \mathrm{d}z \, |\chi_0(z)|^2 = 1,$$

respectively. We will assume that at $\varepsilon \leqslant \varepsilon_F$ only one discrete quantum state ε_0 is filled in the surface potential well (see figure 2). The solution $\varphi_{00\text{sur}}(\mathbf{r})$ of (A.6) describes the wave function of the surface states near an ideal impermeable interface. The correction to the wave function (A.6) linear in the constant g can be expressed by means of the Green's function $G^+(\mathbf{r}, \mathbf{r}'; \varepsilon)$ of the unperturbed surface states [13] in the field of the potential $V_{\text{sur}}(z)$ near the impenetrable interface.

To leading order in the constant g the functions $\psi_1(\mathbf{r})$ and $\varphi_1(\mathbf{r})$ can be written as

$$\varphi_{0\text{sur}}(\mathbf{r}) = \varphi_{00\text{sur}}(\mathbf{r}) + \varphi_{00\text{sur}}(\mathbf{r}_0) g \int \mathrm{d}\mathbf{r}' D(\mathbf{r}' - \mathbf{r}_0) G^+(\mathbf{r}, \mathbf{r}'; \varepsilon). \tag{A.9}$$

The retarded Green's function of the surface states is given by

$$G^+(\mathbf{r}, \mathbf{r}'; \varepsilon) = \chi_0(z) \chi_0^*(z') G_{2D}^+(\boldsymbol{\rho} - \boldsymbol{\rho}'; \varepsilon - \varepsilon_0) \tag{A.10}$$

with

$$G_{2D}^+(\boldsymbol{\rho}; \varepsilon) = \frac{1}{(2\pi)^2} \int_{-\infty}^\infty \mathrm{d}^2 q \frac{\mathrm{e}^{\mathrm{i}\mathbf{q}\boldsymbol{\rho}}}{\varepsilon - \varepsilon_{2D}(\mathbf{q}) + \mathrm{i}0}. \tag{A.11}$$

The wave function for the electrons that are transmitted through the barrier $\psi_{\text{tr}}(\mathbf{r})$ can be found along the lines described in [23, 24]. Taking the FT of the unknown function $\psi_{\text{tr}}(\mathbf{r})$ in the half-space $z < 0$ (figure 2)

$$\psi_{\text{tr}}(\boldsymbol{\rho}, z) = \int_{-\infty}^\infty \mathrm{d}\boldsymbol{\kappa}' \, \mathrm{e}^{\mathrm{i}\boldsymbol{\kappa}'\boldsymbol{\rho}} \Phi(\boldsymbol{\kappa}', z) \tag{A.12}$$

and substituting this in the Schrödinger equation

$$\left(\varepsilon_{2D} \left(\frac{\hbar\partial}{\mathrm{i}\partial\boldsymbol{\rho}} \right) + \frac{\hbar^2 \partial^2}{2m_z \partial z^2} \right) \psi_{\text{tr}}(\mathbf{r}) + \varepsilon \psi_{\text{tr}}(\mathbf{r}) = 0, \quad z < 0 \tag{A.13}$$

we find for the Fourier component $\Phi(\boldsymbol{\kappa}', z)$ a solution corresponding to a propagating wave along the z direction

$$\Phi(\boldsymbol{\kappa}', z) = \Phi(\boldsymbol{\kappa}', 0) \exp\left(-\mathrm{i}k_z' z \right), \quad z \leqslant 0 \tag{A.14}$$

with $k_z' = \sqrt{2m_z(\varepsilon - \varepsilon_{2D}(\boldsymbol{\kappa}'))}/\hbar$. In order to obtain the waves diverging from the contact and to satisfy the boundary condition (8) we must take $\mathrm{Im}\, k_z' < 0$ at $\varepsilon_{2D}(\boldsymbol{\kappa}') > \varepsilon$. From the simplified

boundary condition (A.5), with known wave function $\varphi_{0\mathrm{sur}}(\mathbf{r})$ (A.6) to zeroth approximation in the constant g, one can find the function $\varphi_{1\mathrm{tr}}(\boldsymbol{\rho}, 0)$ in the plane of interface $z = 0$. Relation (A.9) gives us $\varphi_{1\mathrm{tr}}(\boldsymbol{\rho}, 0)$ to first approximation in the small constant g,

$$
\varphi_{1\mathrm{tr}}(\boldsymbol{\rho}, 0) = -\frac{\hbar^2}{2m_z f(\boldsymbol{\rho})\sqrt{L_x L_y}} \, \mathrm{e}^{\mathrm{i}\kappa\rho} \chi'_{0z}(+0) \left[1 + g \int_{-\infty}^{\infty} \mathrm{d}\boldsymbol{\rho}' \int_0^{\infty} \mathrm{d}z' D_0(\boldsymbol{\rho}' - \boldsymbol{\rho}_0, z') \left| \chi_0(z') \right|^2 \right.
$$
$$
\left. \times \mathrm{e}^{\mathrm{i}\kappa\rho'} G_{2\mathrm{D}}^+ \left(\boldsymbol{\rho} - \boldsymbol{\rho} - '; \varepsilon - \varepsilon_0 \right) \right]. \tag{A.15}
$$

The inverse FT allows us to express $\Phi(\boldsymbol{\kappa}', 0)$ in terms of the known function $\varphi(\boldsymbol{\rho}, 0)$

$$
\Phi(\boldsymbol{\kappa}', 0) = \frac{1}{(2\pi)^2} \int_{-\infty}^{\infty} \mathrm{d}\boldsymbol{\rho}' \, \mathrm{e}^{-\mathrm{i}\kappa'\rho'} \varphi(\boldsymbol{\rho}', 0) \tag{A.16}
$$

and we finally obtain the wave function for the transmitted electrons

$$
\psi_{\mathrm{tr}}(\boldsymbol{\rho}, z) = \frac{1}{(2\pi)^2 U_0} \int_{-\infty}^{\infty} \mathrm{d}\boldsymbol{\rho}' \int_{-\infty}^{\infty} \mathrm{d}\boldsymbol{\kappa}' \varphi_{1\mathrm{tr}}(\boldsymbol{\rho}', 0) \, \mathrm{e}^{\mathrm{i}\kappa'(\rho - \rho') - \mathrm{i}k_z'|z|}, \tag{A.17}
$$

where $\varphi_{1\mathrm{tr}}(\boldsymbol{\rho}', 0)$ is given by equation (A.15).

Appendix B. Asymptotes for $\rho \to \infty$ of the Green function $G_{2\mathrm{D}}^+(\rho; \varepsilon)$ of two-dimensional electrons with an arbitrary Fermi contour

After replacing the integration over the 2D vector $\mathbf{q}$ by integrations over the energy $\varepsilon' = \varepsilon_{2\mathrm{D}}(\mathbf{q})$ and over the arc length $l_{\mathbf{q}}$ of the constant energy contour, equation (A.11) takes the form

$$
G_{2\mathrm{D}}^+(\rho; \varepsilon) = \frac{1}{(2\pi)^2} \int_0^{\infty} \frac{\Lambda(\varepsilon', \boldsymbol{\rho})\mathrm{d}\varepsilon'}{\varepsilon - \varepsilon' + \mathrm{i}0}, \tag{B.1}
$$

where

$$
\Lambda(\varepsilon', \boldsymbol{\rho}) = \oint_{\varepsilon' = \varepsilon_{2\mathrm{D}}(\mathbf{q})} \frac{\mathrm{d}l_{\mathbf{q}}}{\hbar v_{\mathbf{q}}} \, \mathrm{e}^{\mathrm{i}\mathbf{q}\rho} \tag{B.2}
$$

and $v_{\mathbf{q}} = |\partial \varepsilon_{2\mathrm{D}}(\mathbf{q})/\hbar \partial \mathbf{q}|$ is the absolute value of the 2D velocity vector. For $\rho \to \infty$ the integral in equation (B.2) can by calculated asymptotically by using the stationary phase method (see e.g. [28]). Let us parameterize the curve $\varepsilon_{2\mathrm{D}}(\mathbf{q}) = \varepsilon'$ by using the angle ϕ in the $q_x q_y$-plane as a parameter, $q_{x,y} = q_{x,y}(\varepsilon', \phi)$. The element of arc length $\mathrm{d}l_{\mathbf{q}}$ can then be expressed as $\mathrm{d}l_{\mathbf{q}} = \sqrt{\dot{q}_x^2 + \dot{q}_y^2} \, \mathrm{d}\phi$ and we obtain

$$
\Lambda_{\mathrm{as}}(\varepsilon', \boldsymbol{\rho}) \simeq \frac{1}{\hbar v_{\mathbf{q}}} \sqrt{\frac{2\pi \left(\dot{q}_x^2 + \dot{q}_y^2 \right)}{\left| \ddot{q}_x \rho_x + \ddot{q}_y \rho_y \right|}} \exp \left[\mathrm{i}\mathbf{q}\rho + \frac{\pi \mathrm{i}}{4} \mathrm{sgn} \left(\ddot{q}_x \rho_x + \ddot{q}_y \rho_y \right) \right] \Bigg|_{\phi = \phi_{\mathrm{st}}} + O\left(\frac{1}{\rho} \right), \tag{B.3}
$$

where the dot over a function denotes differentiation with respect to ϕ. The stationary phase point $\phi = \phi_{\mathrm{st}}(\varepsilon')$ is defined by the equation

$$
\dot{q}_x \rho_x + \dot{q}_y \rho_y |_{\phi = \phi_{\mathrm{st}}} = 0. \tag{B.4}
$$

Note that the total derivative of the energy $\varepsilon_{2\mathrm{D}}(\mathbf{q}) = \varepsilon$ with respect to ϕ is equal to zero because this energy is the same for all directions ϕ of the vector $\mathbf{q}$,

$$\dot{\varepsilon}_{2\mathrm{D}}(\mathbf{q}) = \hbar v_x \dot{q}_x + \hbar v_y \dot{q}_y = 0. \tag{B.5}$$

Equation (B.5) provides a relation between the derivatives $\dot{q}_{x,y}$ and the components of the velocity $v_{x,y}$. Introducing the curvature $K(\mathbf{q})$ of the constant energy contour $\varepsilon_{2\mathrm{D}}(\mathbf{q}) = \varepsilon'$

$$K(\mathbf{q}) = \frac{\ddot{q}_y \dot{q}_x - \ddot{q}_x \dot{q}_y}{\left(\dot{q}_x^2 + \dot{q}_y^2\right)^{3/2}}, \tag{B.6}$$

equations (B.3) and (B.4) can be rewritten in the form

$$\Lambda_{\mathrm{as}}(\varepsilon', \boldsymbol{\rho}) \simeq \sqrt{2\pi} \left. \frac{\exp\left[\mathrm{i}\mathbf{q}\boldsymbol{\rho} + \frac{\pi \mathrm{i}}{4}\mathrm{sgn}K(\mathbf{q})\right]}{\hbar v_{\mathbf{q}}\sqrt{\rho\,|K(\mathbf{q})|}} \right|_{\mathbf{q}=\mathbf{q}_{\mathrm{st}}} + O\left(\frac{1}{\rho}\right) \tag{B.7}$$

and

$$\left.\frac{v_x}{v_y}\right|_{\mathbf{q}=\mathbf{q}_{\mathrm{st}}} = \frac{\rho_x}{\rho_y}, \tag{B.8}$$

where $\mathbf{q}_{\mathrm{st}} = (q_x(\phi_{\mathrm{st}}), q_y(\phi_{\mathrm{st}}))$. The equality (B.8) is satisfied when the velocity $\mathbf{v}_{\mathbf{q}_{\mathrm{st}}}$ is parallel or antiparallel to the vector $\boldsymbol{\rho}$. We choose the solution of equation (B.8) with $\mathbf{v}_{\mathbf{q}_{\mathrm{st}}} \parallel \boldsymbol{\rho}$ that corresponds to the outgoing waves. Generally, for arbitrarily complicated (non-convex) constant energy contours there can be many solutions $\mathbf{q}_{\mathrm{st}}^{(s)}$ ($s = 1, 2, \ldots$) and in equation (B.7) one must sum over all of them.

In order to calculate the integral over ε' in equation (B.1) we consider the integral J_C along the closed contour C shown in figure B.1,

$$J_C = \frac{1}{(2\pi)^{3/2}} \lim_{R \to \infty} \int_C \frac{\Lambda_{\mathrm{as}}(\varepsilon', \boldsymbol{\rho})\mathrm{d}\varepsilon'}{\varepsilon - \varepsilon' + \mathrm{i}0}. \tag{B.9}$$

There is only one pole $\varepsilon = \varepsilon' + \mathrm{i}0$ inside C and this integral is equal to

$$J_C = \lim_{R \to \infty} \left\{ \int_0^R + \int_{C_R} + \int_{\mathrm{i}R}^0 \mathrm{d}\varepsilon' \right\} = 2\pi \mathrm{i} \Lambda_{\mathrm{as}}(\varepsilon, \boldsymbol{\rho}). \tag{B.10}$$

The first integral in (B.10) for $R \to \infty$ is the desired integral in equation (B.1). The second integral along the arc C_R vanishes for $R \to \infty$ if $\mathrm{Re}(\mathrm{i}\mathbf{q}\boldsymbol{\rho}) < 0$ in the first quadrant of the plane of the complex variable $\varepsilon' = \varepsilon_1 + \mathrm{i}\varepsilon_2$. The third integral in (B.10) along the complex axis $\mathrm{i}\varepsilon_2$ rapidly decreases with increasing distance ρ, more rapidly than the first one because of the exponential dependence of the integrand.

The last two statements can be proven explicitly for an isotropic dispersion law of 2D charge carriers. For a circular contour of constant energy $\varepsilon = (\hbar\kappa)^2/2m$, $\varepsilon' = (\hbar q')^2/2m$, $v = \hbar q'/m$, $K(\mathbf{q}) = 1/q'$, $\mathbf{q}_{\mathrm{st}}\boldsymbol{\rho} = q'\rho$. Replacing the integration over ε' by integration over q' we obtain

$$J_C = \lim_{R \to \infty} \left\{ \int_0^R + \int_{C_R} + \int_{\mathrm{i}R}^0 \mathrm{d}q' \right\} = \frac{m}{\pi \hbar^2 \sqrt{\rho}} \int_C \frac{\sqrt{q'}\,\mathrm{d}q'}{\kappa^2 - q'^2 + \mathrm{i}0} \exp\left[\mathrm{i}q'\rho + \frac{\pi \mathrm{i}}{4}\right]. \tag{B.11}$$
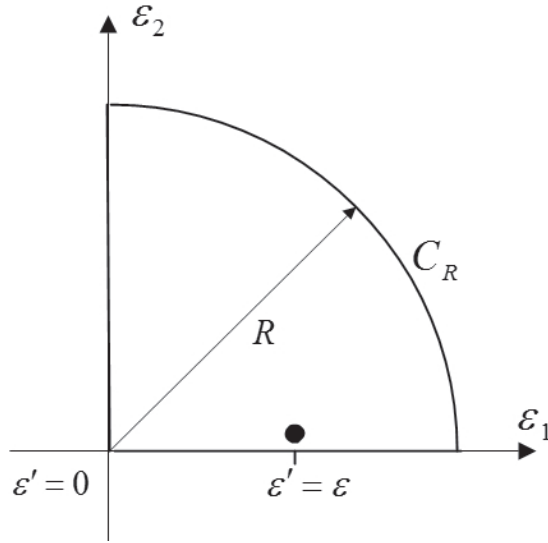
Figure B.1. Contour of integration used in equations (B.9) and (B.11). The black dot shows the position of the pole of the integrand.

For the integral (B.11) we use the same contour as for integral (B.9) (see figure B.1). Let us replace the integration variable q' in the second integral along the circle quarter C_R by $q' = Re^{i\chi}$. Then it is easy to estimate the absolute value of the integral as

$$\left| \int_{C_R} \frac{\sqrt{q'}\, dq'}{\kappa^2 - q'^2 + i0} \exp\left[iq'\rho + \frac{\pi i}{4} \right] \right| < \frac{1}{\sqrt{R}} \int_0^{\pi/2} d\chi\, e^{-R\rho \sin\chi} \tag{B.12}$$

$$< \frac{1}{\sqrt{R}} \int_0^{\pi/2} d\chi\, e^{-2R\rho\chi/\pi} = \frac{\pi}{2\rho R^{3/2}} \left(1 - e^{-R\rho} \right) \underset{R\to\infty}{\to} 0.$$

After substituting $\xi = -iq'$ the third integral along the imaginary axis takes the form

$$\lim_{R\to\infty} \frac{1}{\sqrt{\rho}} \int_{iR}^0 \frac{\sqrt{q'}\, dq'}{\kappa^2 - q'^2 + i0} \exp\left[iq'\rho + \frac{\pi i}{4} \right] = \frac{1}{\sqrt{\rho}} \int_0^\infty \frac{\sqrt{\xi}\, e^{-\xi\rho}\, d\xi}{\kappa^2 + \xi^2}$$

$$= \frac{\pi}{\sqrt{\kappa\rho}} \left[\cos\kappa\rho \left(1 - 2C\left(\sqrt{\kappa\rho}\right) \right) + \sin\kappa\rho \left(1 - 2S\left(\sqrt{\kappa\rho}\right) \right) \right]$$

$$\underset{\rho\to\infty}{\longrightarrow} \frac{\sqrt{\pi}}{2\kappa^2\rho^2} + O\left(\frac{1}{\rho^3} \right), \tag{B.13}$$

where $C(z)$ and $S(z)$ are the Fresnel integrals

$$\begin{Bmatrix} C(z) \\ S(z) \end{Bmatrix} = \sqrt{\frac{2}{\pi}} \int_0^z dt \begin{Bmatrix} \cos t^2 \\ \sin t^2 \end{Bmatrix}. \tag{B.14}$$

Finally we obtain the following asymptotic expression for the Green function:

$$G_{2D}^+(\boldsymbol{\rho}; \varepsilon) \simeq \frac{i}{\sqrt{2\pi}} \frac{\exp\left[i\mathbf{q}\boldsymbol{\rho} + \frac{\pi i}{4} \operatorname{sgn} K(\mathbf{q}) \right]}{\hbar v_\mathbf{q} \sqrt{\rho\, |K(\mathbf{q})|}} \Bigg|_{\mathbf{q} = \mathbf{q}_{st}(\varepsilon, \phi_{st})}, \qquad \rho \to \infty. \tag{B.15}$$

References

[1] Crommie M F, Lutz C P and Eigler D M 1993 *Nature* **363** 524
Crommie M F, Lutz C P and Eigler D M 1993 *Science* **262** 218

[2] Petersen L *et al* 2000 *J. Electron Spectrosc. Relat. Phenom.* **109** 97

[3] Simon L, Bena C, Vonau F, Cranney M and Aube D 2011 *J. Phys. D: Appl. Phys.* **44** 464010

[4] Friedel F 1958 *Nuovo Cimento* **7** 287

[5] Petersen L *et al* 1998 *Phys. Rev.* B **57** R6858

[6] Vonau F, Aubel D, Gewinner G, Pirri C, Peruchetti J C, Bolmont D and Simon L 2004 *Phys. Rev.* B **69** R081305

[7] Sprunger P T, Petersen L, Plummer E W, Lagsgaard E and Besenbacher F 1997 *Science* **275** 1764

[8] Petersen L, Schaefer B, Lagsgaard E, Stensgaard I and Besenbacher F 2000 *Surf. Sci.* **457** 319–25

[9] Fujita D, Xu M, Onishi K, Kitahara M and Sagisaka K 2004 *J. Electron. Microsc.* **53** 177

[10] Briner B G, Hofmann Ph, Doering M, Rust H-P, Plummer E W and Bradshaw A M 1997 *Europhys. Lett.* **39** 67

[11] Petersen L, Laitenberger P, Lagsgaard E and Besenbacher F 1998 *Phys. Rev.* B **58** 5361

[12] Kralj M, Milun M and Pervan P 2004 *Surf. Sci.* **557** 208

[13] Avotina Ye S, Kolesnichenko Yu A, Otte A F and Ruitenbeek J M 2006 *Phys. Rev.* B **74** 085411

[14] Avotina Ye S, Kolesnichenko Yu A, Roobol S B and Ruitenbeek J M 2008 *Low Temp. Phys.* **34** 207

[15] Weismann A, Wenderoth M, Lounis S, Zahn P, Quaas N, Ulbrich R G, Dederichs P H and Blügel S 2009 *Science* **323** 1190

[16] Lounis S, Zahn P, Weismann A, Wenderoth M, Ulbrich R G, Mertig I, Dederichs P H and Blügel S 2011 *Phys. Rev.* B **83** 035427

[17] Avotina Ye S, Kolesnichenko Yu A and Ruitenbeek J M 2010 *Low Temp. Phys.* **36** 849
Avotina Ye S, Kolesnichenko Yu A and Ruitenbeek J M 2010 *Fiz. Nizk. Temp.* **36** 1066

[18] Tersoff J and Hamann D 1983 *Phys. Rev. Lett.* **50** 1998
Tersoff J and Hamann D 1985 *Phys. Rev.* B **31** 805

[19] Bardeen J 1961 *Phys. Rev. Lett.* **6** 57

[20] Fiete G A and Heller E J 2003 *Rev. Mod. Phys.* **75** 933

[21] Hofer W A, Foster A S and Shluger A L 2003 *Rev. Mod. Phys.* **75** 1287

[22] Blanco J M, Flores F and Perez R 2006 *Prog. Surf. Sci.* **81** 403

[23] Kulik I O, Mitsai Yu N and Omel'yanchuk A N 1974 *Sov. Phys.—JETP* **39** 514
Kulik I O, Mitsai Yu N and Omel'yanchuk A N 1974 *Zh. Eksp. Theor. Phys.* **66** 1051

[24] Avotina Ye S, Kolesnichenko Yu A, Omelyanchouk A N, Otte A F and Ruitenbeek J M 2005 *Phys. Rev.* B **71** 115430

[25] Lifshits I M, Azbel' M Ya and Kaganov M I 1973 *Electron Theory of Metals* (New York: Colsultants Bureau)

[26] Khotkevych N V, Kolesnichenko Yu A and Ruitenbeek J M 2013 *Low Temp. Phys.* **39** 299

[27] Guggenheimer H W 1997 *Differential Geometry* (General Publishing Company)

[28] Maslov V P and Fedoriuk M V 1981 *Semi-Classical Approximation in Quantum Mechanics* (Dordrecht: Reidel)

[29] Rabinowitz S 1997 *Missouri J. Math. Sci.* **9** 23